FRANCISZEK ŚCIGALSKI*), BEATA JĘDRZEJEWSKA, MAREK PIETRZAK, WALDEMAR WIŚNIEWSKI, JERZY PĄCZKOWSKI

University of Technology and Life Sciences
Faculty of Chemical Technology and Engineering
Seminaryjna 3, 85-326 Bydgoszcz, Poland

Silver-nanoparticles immobilized initiators and co-initiators for free radical polymerization

Summary — The specific properties of silver-nanoparticles immobilized initiator and co-initiators for free radical polymerization have been described. The silver-nanoparticles immobilized mercaptobenzophenone (Bp-MPCs) photoinitiates free radical polymerization in both UV and visible regions. The photoinitiation ability of Bp-MPCs in visible region, *e.g.* in the region in which benzophenone chromophore does not absorb a light, indicates a possible two-photon action even at low incident light intensity. The co-initiation process caused by silver-nanoparticles immobilized mercaptoamino acids (MA-MPCs) is more efficient in comparison to co-initiation observed for corresponding free mercaptoamino acid. This behavior can be attributed the specific interaction of sulfur electrons with surface plasmon electrons that make an electron transfer from mercaptoamino acid to excited electron acceptor more efficient, or to a high concentration of the electron donor in the ligand shell.
Keywords: silver-nanoparticles, free radical polymerization, photoinitiators, mercaptobenzophenones, mercaptoamino acids.

MODYFIKOWANE NANOCZĄSTKI SREBRA JAKO INICJATORY I KOINICJATORY POLIMERYZACJI RODNIKOWEJ

Streszczenie — Otrzymano nanocząstki srebra stabilizowane pochodnymi merkaptobenzofenonu (Bp-MPCs) oraz merkaptoaminokwasami (MA-MPCs) (rys. 1—4). Zbadano przebieg fotoinicjowania polimeryzacji triakrylanu 2-etylo-2-(hydroksymetylo)-1,3-propanodiolu (TMPTA) za pomocą zsyntetyzowanego fotoinicjatora Bp-MPCs działającego w zakresie promieniowania UV lub światła widzialnego, w układzie z koinicjatorem lub bez (rys. 5—8). Efektywność inicjowania polimeryzacji w obecności koinicjatora w postaci MA-MPCs jest większa niż w przypadku użycia odpowiednich merkaptoaminokwasów, gdyż nanocząstki srebra stabilizowane merkaptoaminokwasami wykazują większą zdolność do oddawania elektronów w procesie polimeryzacji PET. Fotoinicjowanie polimeryzacji TMPTA przez Bp-MPCs w obszarze widzialnym, tj. w obszarze w którym pochodna benzofenonu nie absorbuje promieniowania, może sugerować występowanie absorpcji dwufotonowej, pomimo małego natężenia padającego promieniowania (100 mW/cm^2).
Słowa kluczowe: nanocząstki srebra, polimeryzacja wolnorodnikowa, fotoinicjatory, merkaptobenzofenony, merkaptoaminokwasy.

The process of photoinitiated polymerization can proceed by the direct photolysis of a precursor which undergoes bond dissociation to provide free radicals. The radicals may also be obtained in bimolecular processes involving either electron or atom transfer reactions [1]. Generally, the components of such initiating systems act as a classical single-phase solution in which the composition is uniform on the molecular scale (solutes are present as single molecules). The second approach involves a polymer chain as the initiator carrier. This applies to both types of initiators — photoinitiators that form free radicals in the photocleavage reaction [2—4] as well as in the bimolecular process [5—7].

The literature, however, does not provide studies of photoinitiators immobilized on noble metal surfaces, known as monolayer — protected clasters (MPCs) [8—10]. MPCs have received much attention recently due to their unique properties which make them ideal candidates for applications in a variety of technologies such as non-linear optics [11] micro-arrays [12], biocompatible coating [13, 14] or the synthesis of polymer brushes [15, 16].

*) To whom correspondence should be addressed: e-mail: scigal@utp.edu.pl

In this paper, the synthesis and characterization of silver nanoparticles immobilized either on mercaptoamino acids (L-cysteine, homocysteine, L-cysteine, *N*-acetyl-L-cysteine and/or L-glutatione) (MA-MPC) or mercaptobenzophenone derivatives (Bp-MPCs) has been presented. The MA-MPC and Bp-MPC nanoparticles were applied as radical polymerization co-initiators and initiators respectively.

EXPERIMENTAL

Materials

The chemicals were of the purest grade available (Sigma, Aldrich) and used as received.

The composition of the polymerization solution was dependent on the type of photoinitiating system applied.

— For benzophenone-functionalized silver nanoparticle electron acceptors (Bp-MPCs) it consisted of 1 mL of 1-methyl-2-pyrrolidinone (MP), 9 mL of 2-ethyl--2-(hydroxymethyl)-1,3-propanediol triacrylate (TMPTA) and an appropriate amount of photoinitiating systems to guarantee maximum photoinitiation efficiency. Blank photochemical experiments were performed for each photoinitiated polymerization using 4-(6-mercaptohexyloxy)benzophenone (c = 0.01 M) dissolved in TMPTA and MP (9:1) mixture.

— For mercaptoamino-acid-functionalized silver nanoparticles (MA-MPCs) acting as co-initiators the polymerizing formulation consisted of 1.5 mL of poly(ethylene glycol)diacrylate (PEGDA, average M_n = 575) and 0.5 mL of H_2O. The dye concentration [5,7-diiodo-3-butoxy-6-fluorone (DIBF)] [17—19]) was $1 \cdot 10^{-3}$ M while MA-MPCs concentration varied from 7.2 to 15.2 mg/2 mL, depending on the type used.

Synthesis

Benzophenone derivative, 4-(6-mercaptohexyloxy)benzophenone, used for silver nanoparticles functionalization was prepared according to the sequence of reaction presented in Scheme A.

4-(6-Mercaptohexyloxy)benzophenone was obtained *via* a three-step synthetic route. The final product was purified by crystallization from ethanol yielding white crystals. ^{1}H NMR [$(CD)_2SO$]; δ 1.1—1.8 (m, 16 H, -CH_2-), δ 2.201—2.238 (t, 1H-SH), δ 4.029—4.088 (t, 2H, PhO-CH_2-), δ 7.044—7.740 (m, 9H, Ar).

Decanethiol-functionalized silver nanoparticles (DT-MPCs) were synthesized applying the single-phase synthesis procedures proposed by Murthy [20]. 1.0 g (5.20 mmol) of $AgNO_3$ was dissolved in 150 mL of absolute ethanol in a round-bottom flask. 1-Decanethiol (0.13 g, 0.75 mmol) was also dissolved in about 3 mL of absolute ethanol and then added to the $AgNO_3$ solution under vigorous stirring. 50 mL of freshly prepared saturated $NaBH_4$ in absolute ethanol was added dropwise to the obtained (milky) solution. The colour of the solution changed to dark brown. The resulting mixture was stirred overnight and then stored at -20 °C for 4 hours. The obtained precipitate was filtered, washed with ethanol, acetone, water and finally with acetone. The dark-brown powder was dissolved in dichloromethane and the solution was filtered with a 0.4 μm pore size Nylaflo membrane filter. The solvent was evaporated under reduced pressure and the resulting dark-brown solid film separated from the walls of the flask with acetone. Finally, the mixture was filtered yielding about 200 mg of graphite-like powder.

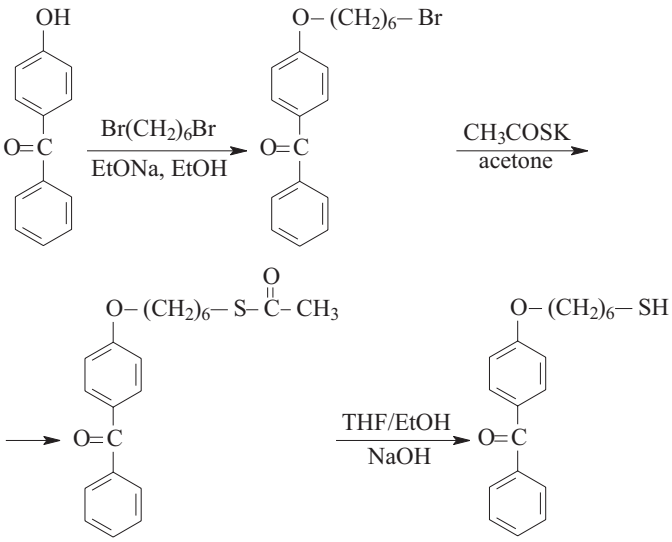

Scheme A. A general route for the synthesis of the precursor used for silver nanoparticles preparation

Functionalization of decanethiol-functionalized silver nanoparticles. Equilibrium place-exchange reaction was performed between DT-MPCs and 4-(6-mercaptohexyloxy)benzophenone. Approximately 200 mg DT-MPCs was dissolved in 50 mL of THF and then 100 mg of 4-(6-mercaptohexyloxy)benzophenone added to the obtained solution. The solution was stirred at ambient temperature for 24 hours, after which the solvent was evaporated under vacuum. The product was washed thoroughly with ethanol to remove unreacted 4-(6-mercaptohexyloxy)benzophenone. The presence of unreacted 4-(6-mercaptohexyloxy)benzophenone in the resulting benzophenone-functionalized silver nanoparticles was monitored using thin layer chromatography.

Mercaptoamino acids-functionalized silver nanoparticles (MA-MPCs). The general procedure of MA-MPCs synthesis was based on modified version of the methodology given by Kang and Kim [21]. The procedure for obtaining cysteine-functionalized MPCs was as follows: 1.7 g (10 mmol) of $AgNO_3$ was dissolved in 250 mL of an ethanol-water mixture (1:1) in a round-bottom flask. 3.36 g of cysteine was dissolved in 100 mL water and the solution added dropwise to the $AgNO_3$ solution. A milky yellow mixture was obtained, to which a

freshly prepared solution of 1.7 g (50 mmol) of $NaBH_4$ in 40 mL of EtOH was added using pressure-equalizing dropping funnel. The resulting dark-brown mixture was stirred overnight and then stored at ≈ -20 °C for 4 hours. The obtained precipitate was filtered, washed with ethanol and acetone. A yield of 1.82 g of dark-brown powder soluble in water was achieved.

Methods of testing

— UV/Vis absorption spectra were obtained using a Varian Cary 3E Spectrophotometer and a MultiSpec 1501 Shimadzu spectrophotometer.

— FT-IR spectra were measured with a use of a Bruker Vector 22 spectrophotometer. The thermogravimetric analysis was performed with a Q-1500 D derivatograph (Hungary).

— NMR spectra were obtained from a Varian Gemini 2000 spectrometer using the solvents indicated.

— The kinetics of free radical polymerization was measured based on measurements of the rate of the heat evolution during polymerization in a cured thin film sample. The measurements were performed by means of photopolymerization exotherms using: (i) photo-DSC apparatus constructed on the basis of a TA Instruments DSC 2010 Differential Scanning Calorimeter (for polymerization in visible region) and (ii) a homemade thin-film calorimeter constructed the basis of the model described by Hoyle *et al.* (for polymerization in UV region) [22, 23]. The single cell calorimeter is based on a thin-film heat flux sensor of antimony-bismuth thermocouples arranged in a sterr-shaped configuration [24]. The irradiation of the polymerization mixture was carried out using the emission of both an Innova 90-4 argon-ion laser (351 and 361 nm lines) and an Omnichrome model 543-500 MA argon-ion laser, which emits two visible light wavelengths at 488 and 514 nm. The average incident power of irradiation was measured with Coherent Model Fieldmaster power meter.

— The rate of polymerization (R_p) in the photo-DSC technique was calculated using formula (1) where dH/dt is the maximum heat flow during the reaction and ΔH_p^{theor} the theoretical enthalpy for a complete conversion of acrylate double bonds. The ΔH_p^{theor} value calculated for acrylic double bond is 78.2 kJ/mol.

$$R_p = \left(\frac{dH}{dt}\right)\frac{1}{\Delta H_p^{theor}} \quad (1)$$

In the case of the polymerization kinetic measurements based on a homemade thin-film calorimeter, the rate of polymerization was calculated as the direct coefficient of linear curve describing the changes of emitted heat for the initial polymerization time.

RESULTS AND DISCUSSION

The target nanoparticles were prepared in a sequence of reactions. The overall reaction route leading to MPC initiators and MPC co-initiators is summarized in Fig. 1. Benzophenone-functionalized silver nanoparticles (Bp-MPCs) were prepared in the reaction sequence start-

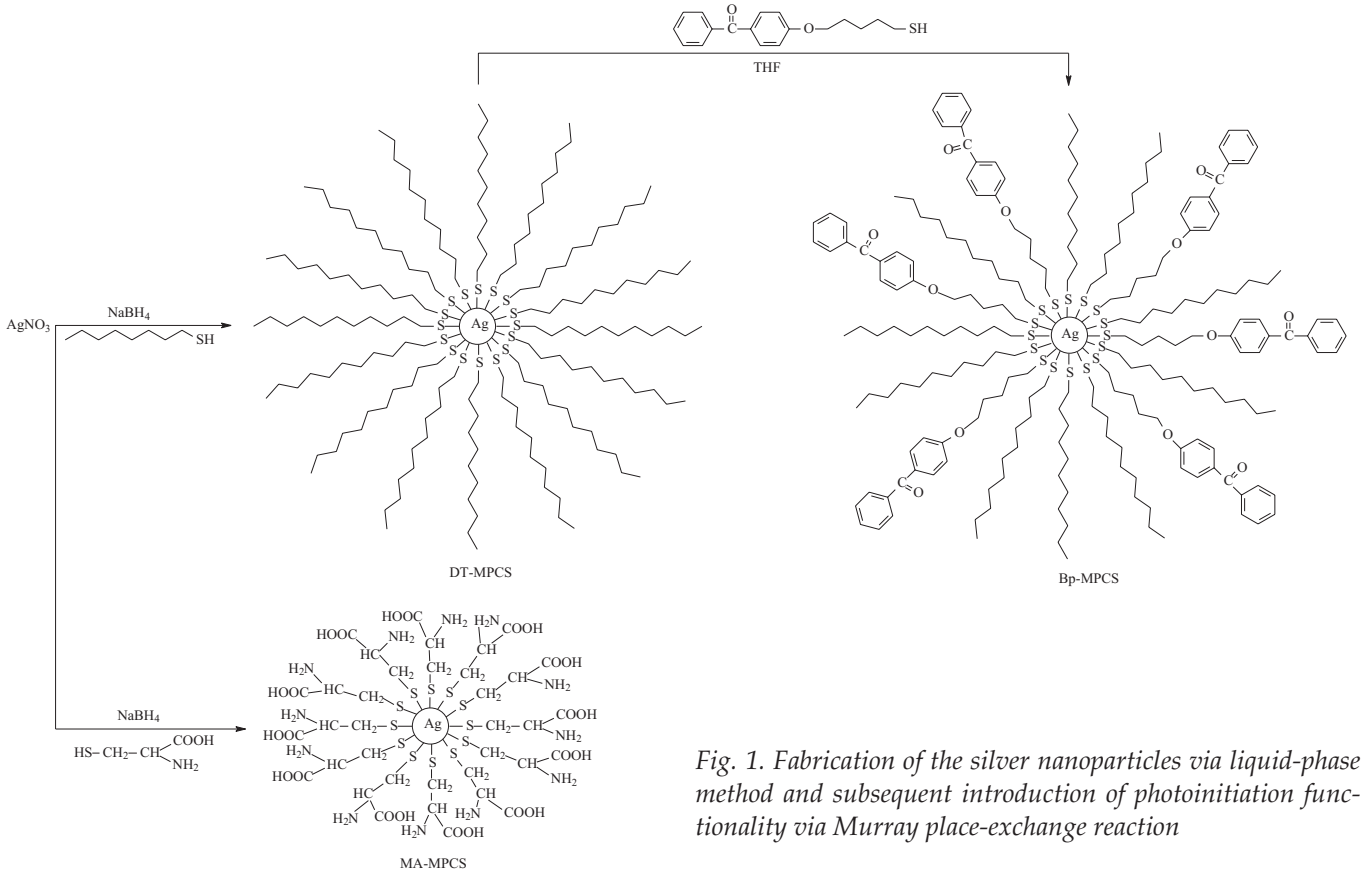

Fig. 1. Fabrication of the silver nanoparticles via liquid-phase method and subsequent introduction of photoinitiation functionality via Murray place-exchange reaction

ing form the synthesis of decanetiol-protected silver claster (DT-MPCs) applying the single-phase synthesis proposed by Murthy, followed by Murray place-exchange reaction [25] (steps a and b, respectively).

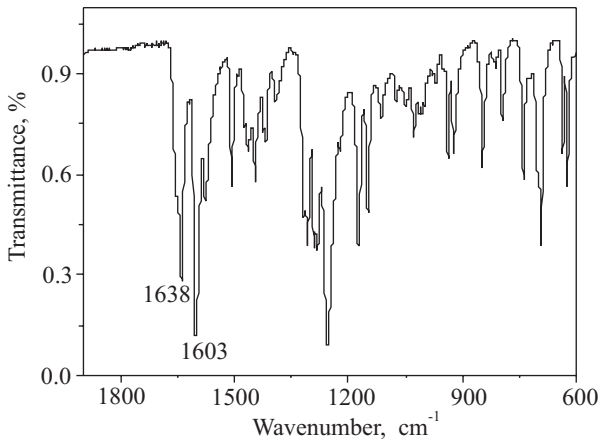

Fig. 2. IR spectra of Bp-MPCs [mixed decanethiol — 4-(6-mercaptohexyloxy)benzophenone silver monolayer-protected clusters] (KBr pellet)

4-(6-Mercaptohexyloxy)benzophenone was used as the substrate for the place-exchange reaction. The final Bp-MPCs were purified using preparative thin layer chromatography. Mercaptoamino acid-functionalized silver nanoparticles (MA-MPCs) were obtained as earlier indicated using modified version of the methodology proposed by Kang and Kim [21].

Infrared spectroscopy of Bp-MPCs (Fig. 2) reveal benzene ring stretching modes at ~1603 cm^{-1} and ~1775 cm^{-1}, as well as a C=O group stretching mode (~1638 cm^{-1}) characteristic for benzophenone. The observed IR spectra is very similar to that recorded for 4-(6-mercaptohexyloxy)benzophenone. These results suggest that the environment in KBr pellets of the chromophores on nanoparticles is similar to that recorded for unbound molecules. Similarly, all mercaptoamino acids-stabilized silver nanoparticles synthesized show stretching and bending modes characteristic for mercaptoamino acids molecules in the IR region.

Thermal decomposition of DT-MPCs (Fig. 3) leads to volatilization of the organic fraction, leaving a silver residue. TGA measurements show a 20 % loss of the organic fraction of DT-MPCs. This result leads to a number of the silver atoms per ligand molecule of about 8. This ratio, according to Murray *et al.* [26] indicate that the ligand place-exchange process has a 1:1 stoichiometry and remains identical after partial exchange of decanetiol on 4-(6-mercaptohexyloxy)benzophenone. Consequently, it can be predicted that 80 atoms of silver claster are stabilized by 10 of both types of ligand molecules (tiolate-Ag ratio equal 0.20). A different situation is observed for mercaptoamino acid — stabilized silver nanoparticles.

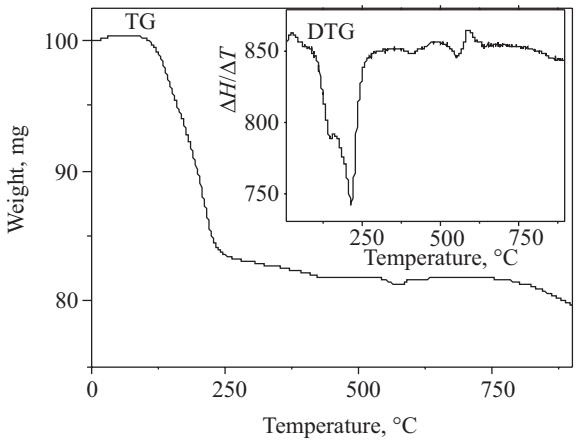

Fig. 3. TG curve of Bp-MPC nanoparticles. Inset: DTG plot for Bp-MPCs

The tiolate-Ag ratio oscillate from about 0.5 to 1.0 depending on the type of mercaptoamino acid used.

Figure 4 shows the electronic absorption spectra of DT-MPCs and Bp-MPCs.

For DT-MPCs a broad strong band at about 430 nm is observed. This band is characteristic for the noble metal plasmon band, whose position is highly dependent on the size and environment of the particles [27, 28]. The place-exchange reaction introducing benzophenone molecules into the MPCs protecting monolayer visibly changes the spectrum. The plasmon absorption band broader and its maximum is slightly shifted to the red. Moreover, a new band appears at about 280 nm. This additional band can be attributed to the presence of benzo-

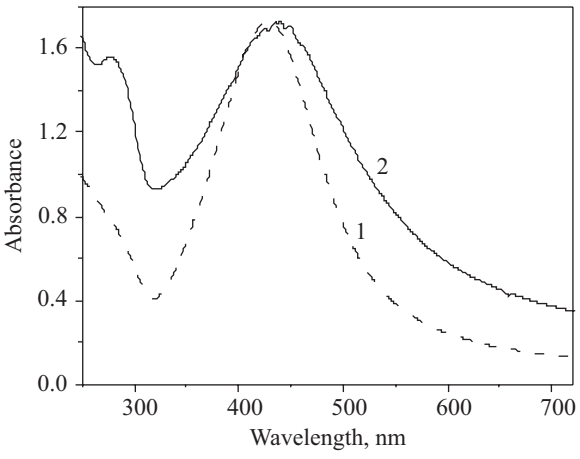

Fig. 4. Electronic absorption spectra of DT-MPCs (1) and Bp-MPCs (2) in CH_2Cl_2 solution

phenone $\pi \rightarrow \pi^*$ transition. The electronic absorption spectra Bp-MPCs also demonstrate a plasmon band localized in the range between 400 and 450 nm characteristic for noble metal nanoparticles.

The photoinitiation ability of the studied photoinitiators and co-inititors was measured using microcalori-

metric methodology. For the Bp-MPC initiator and the TMPTA with MP (9:1) mixture measurements of the kinetics of polymerization were carried out by measuring the polymerization heat evolution of the sample, irradiated with an Innova 90-4 argon-ion laser (351 and 361 nm lines). The MA-MPC co-initiation ability was tested using DIBF — the xanthene dye described by Neckers [17—19]. The free radical polymerization kinetics was studied using a polymerization solution composed of 1.5 mL of poly(ethylene glycol)diacrylate (PEGDA) and 0.5 mL of H_2O. The dye concentration was $1 \cdot 10^{-3}$ M and MA-MPC concentration was varied from 7.2 to 15.2 mg/2 mL. The amount of MA-MPCs used as co-initiator was established on the basis of TG measurements. From the degree of loss of the organic fraction, a molar fraction of mercaptoamino acid in mg of MA-MPCs was established thereby enabling the concentration of the mercaptoamino acid expressed in mol/L (0.1 mol/L for all cases) to be evaluated.

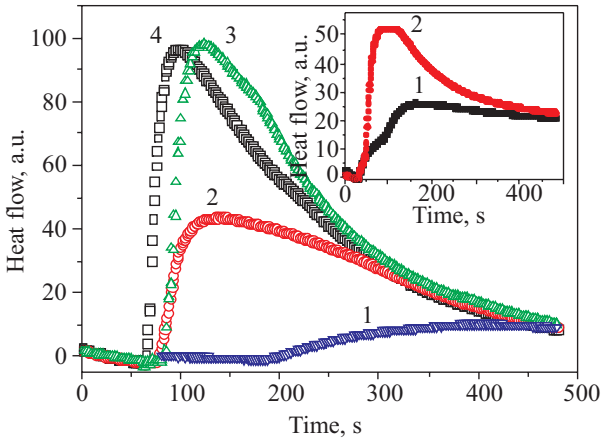

Fig. 5. The family of the photopolymerization kinetic traces recorded for polymerization of the 2-ethyl-2-(hydroxymethyl)-1,3-propanediol triacrylate (TMPTA; 0.9 mL) in the presence of the 1-methyl-2-pyrrolidinone (MP; 0.1 mL) initiated by Bp-MPCs (c = 1.67 mg/mL) irradiated by 351 and 361 nm emission of an Innova 90-4 argon-ion laser. Light intensity was I_a = 60 mW/cm². The electron donors (c = 0.1 M): (1) none, (2) ethyl 4-dimethylaminobenzoate, (3) 4-(dimethylamino)benzonitrile, (4) N-phenylglycine. Inset: Comparison of the initial rates of polymerization photoinitiated by either (1) Bp-MPCs (c = 0.3 mg/mL) or (2) 4-(6-mercaptohexyloxy)benzophenone (c = 0.3 mg/mL) in the presence of ethyl 4-dimethylaminobenzoate (c = 0.1 M)

Several combinations of Bp-MPCs with various electron donors (EDs) were tested as photoinitiating systems and compared with corresponding benzophenone-EDs systems. Typical photoinitiated polymerization curves are presented in Figure 5.

In the presence of commonly applied electron donors, Bp-MPCs show high photoinitiation ability. Blank photochemical experiments were performed for each photoinitiated polymerization with 4-(6-mercaptohexyloxy)benzophenone (*c* = 0.01 M) dissolved in TMPTA-MP mixture and used as reference for all photopolymerization measurements initiated by Bp-MPCs.

An analysis of the kinetic curves presented in Figure 5 indicates that only Bp-MPCs initiate polymerization at a very low rate. The addition of a co-initiator to the polymerizing mixture increases the efficiency of initiation of radical polymerization. However a comparison of the initial rates of polymerization photoinitiated by either Bp-MPCs or 4-(6-mercaptohexyloxy)benzophenone in the presence of ethyl 4-dimethylaminobenzoate (the electron donor) reveals that the polymerizating composition containing Bp-MPCs as light absorber shows a slightly lower photoinitiation ability (see Figure 5 inset and [29]).

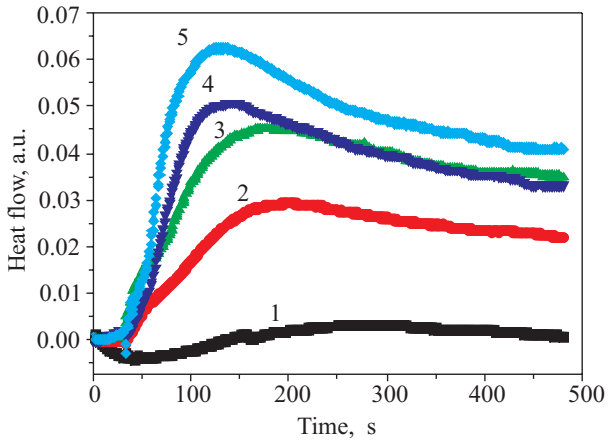

Fig. 6. The family of the photopolymerization kinetic traces recorded for polymerization of the 2-ethyl-2-(hydroxymethyl)-1,3-propanediol triacrylate (TMPTA; 0.9 mL) in the presence of the 1-methyl-2-pyrrolidinone (MP; 0.1 mL) initiated by Bp-MPCs (c = 1.67 mg/mL) irradiated at 488 nm (an Omnichrome argon-ion laser). Light intensities: (1) 20 mW/cm², (2) 40 mW/cm², (3) 60 mW/cm², (4) 100 mW/cm², (5) 130 mW/cm². The electron donors (c = 0.1 M): N-phenylglycine

Unexpectedly, Bp-MPCs initiate polymerization in the presence of several co-initiators when the polymerizing mixture is irradiated at 488 nm (Fig. 6).

This unexpected behavior can be attributed to the specific properties of chromophore in noble metal nanoparticles, described by Perry *et al.* [30] where nanoparticles possessing a chromophore in the stabilizing core show a huge two-photon cross section per-particle. This, in turn, indicates the activation of these particles as two-photon initiators at relatively low light intensity.

Studies on the relationship between the rate of polymerization and irradiation intensity may provide evidence verifying the two-photon hypothesis involved during the photoinitiation under irradiation at 488 nm.

From the kinetic point of view, the mechanism describing photoinitiated polymerization *via* PET process can be presented as follows:

Reaction	Rate	
$Chr + h\nu \longrightarrow Chr^*$	$I_a\Phi_R$ (for one-photon absorption)	(2)
$Chr^* + ED \longrightarrow R^\bullet$	$(I_a)^2\Phi_R$ (for two-photon absorption)	(2a)
$R^\bullet + M \longrightarrow RM^\bullet$		
$RM^\bullet + nM \longrightarrow RM_{n+1}$	$k_p[M][R^\bullet]$	(3)
$RM_n^\bullet + RM_m^\bullet \longrightarrow RM_{n+m}R$	$k_t[R^\bullet]^2$	(4)

where: *Chr — the absorbing light chromophore (in this case silver-nanoparticle), ED — the electron donor, I_a — absorbed light intensity, Φ_R — the quantum yield for initiation, [M] — the monomer concentration, k_p, k_t — the propagation and termination rates constants, respectively.*

For a steady-state condition, $k_t[R^\bullet]^2 = I_a\Phi_R$ for a one-photon initiation and $k_t[R^\bullet]^2 = (I_a)^2\Phi_R$ for two-photon reaction can be assumed.

Thus, basing on these assumptions, the concentration of free radicals $[R^\bullet]$ can be expressed as follows:

$$[R^\bullet] = \sqrt{\frac{I_a\Phi_R}{k_t}}$$ for one-photon initiation and

$$[R^\bullet] = I_a\sqrt{\frac{\Phi_R}{k_t}}$$ for two-photon initiation, respectively.

Consequently, the rate of photoinitiated polymerization (R_p) for both cases is described by the equations:

$$R_p = k_p[M]\sqrt{\frac{I_a\Phi_R}{k_t}} \quad (5a)$$

for one-photon process (5a) and

$$R_p = k_p[M]I_a\sqrt{\frac{\Phi_R}{k_t}} \quad (5b)$$

for two-photon photoinitiated polymerization (5b), respectively.

Form the equations derived above it is evident that, assuming a typical bimacromolecular polymerization termination process for multifunctional acrylates, quite different relationships between the rate of polymerization and irradiation intensity for both cases are obtained. For one-photon initiation process, a linear dependence of the rate of polymerization on the square root of irradiation intensity [eq. (5a)] is observed, while in the case of two-photon reaction the rate of polymerization is a linear function of the light intensity [eq. (5b)]. The kinetic measurement results obtained for photoinitiated polymerization by Bp-MPCs under irradiation at 488 nm are shown in Fig. 7.

The data shown in Fig. 7 clearly demonstrate the kinetics predicted for two-photon photoinitiated polymerization. It should be noted that when 2-ethyl-2-(hydroxymethyl)-1,3-propanediol triacrylate (TMPTA) is initiated by visible-light initiators, it displays almost exclusively a typical linear relationship between the rate of polymerization and square root of irradiation intensity, *i.e.* demonstrates typical one-photon type of photoinitiation [31].

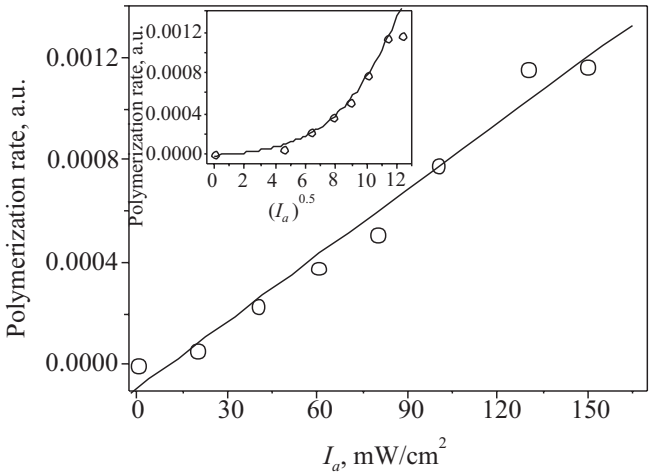

Fig. 7. The relationship between the rate of polymerization and irradiation intensity. Inset: The relationship between the rate of polymerization and square root of irradiation intensity

Bp-MPCs are a highly absorbing species. It is practically not possible to measure their molar absorption coefficient. The value that characterizes Bp-MPC absorption properties, instead, might be the absorbance established for Bp-MPCs solution (at λ_{max}) with a concentration of 1 g/L. For the tested Bp-MPCs this value is equal to: 52.86 and 22.63 at 428 nm and 361 nm (λ_{max}), respectively.

The concentration of the photoinitiator itself also plays a key role in photopolymerization. In conventional UV-Vis photopolymerization R_p increases with an increase in the concentration of the initiator up to a certain level, then it decreases rapidly. This behavior is attributed to the "internal filter effect", which is more significant for photoinitiators with a high molar absorption coefficient [32—34]. The kinetic curves recorded for photoinitiated polymerization at different Bp-MPC concentrations (in mg/mL of formulation) are presented in Fig. 8.

The data shown in Fig. 8 show that, there is essentially no concentration of Bp-MPCs that effects the initial rates of polymerization. There are, however, some differences observed in kinetic curve shape. For this specific behavior it is hard to find a reasonable explanation. There are some observations and facts (Fig. 9) that are characteristic for MA-MPCs acting as co-initiators. Firstly, they do not photoinitiate polymerization without an electron acceptor, and secondly the co-initiation efficiency of MA-MPCs is higher in comparison to corresponding free mercapto-amino acids.

In summary, we have demonstrated the specific properties of silver-nanoparticles immobilized initiator and co-initiators for free radical polymerization. The silver-nanoparticles immobilized benzophenone photoinitiates free radical polymerization in both UV and visible regions. The photoinitiation ability of Bp-MPCs in visible region suggests a possible two-photon action even at low incident light intensity. The co-initiation process by

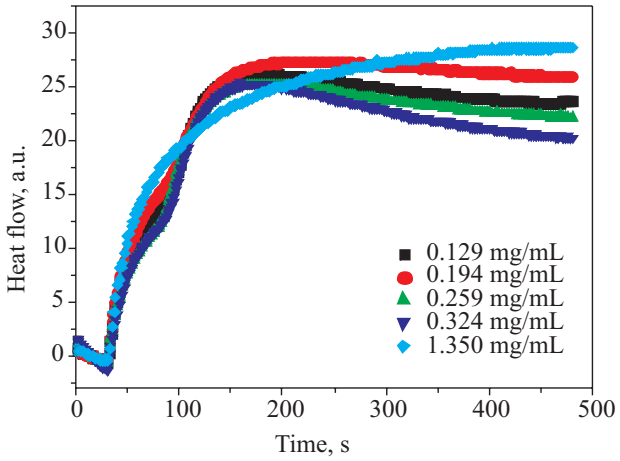

Fig. 8. The family of kinetic curves recorded during the measurements of the flow of heat for the photoinitiated polymerization of the 2-ethyl-2-(hydroxymethyl)-1,3-propanediol triacrylate (TMPTA; 0.9 mL) in the presence of the 1-methyl-2-pyrrolidinone (MP; 0.1 mL) initiated by Bp-MPCs at its various concentrations. As electron donor ethyl 4-(N,N-dimethylamino)benzoate was used (c = 0.1 M). Irradiation at 351 and 361 nm, I_a = 70 mW/cm²

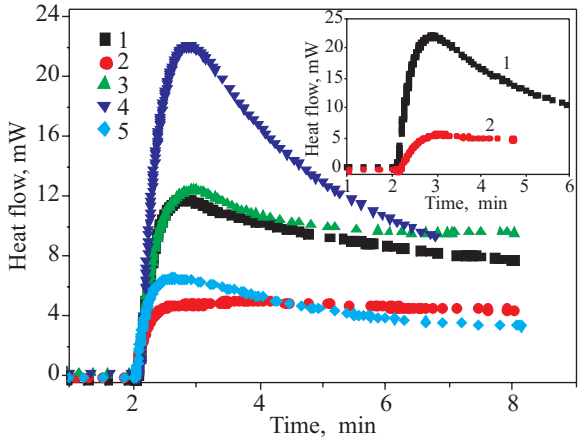

Fig. 9. The family of the photopolymerization kinetic traces recorded for polymerization of the poly(ethylene glycol)diacrylate (PEGDA) and H_2O (3:1) mixture photoinitiated using 5,7-diiodo-3-butoxy-6-fluorone (DIBF) (c = 10^{-3} M) irradiated by 488 nm emission of an argon ion laser. Light intensity: I_a = 60 mW/cm². The MPCs electron donors (concentration of mercaptoamino acid calculated from tiolate-Ag ratio, c = 0.03 M): (1) L-gluthatione-MPCs (c = 8.4 mg/2 mL), (2) L-cystine-MPCs (c = 4.3 mg/2 mL), (3) L-cysteine-MPCs (c = 4.3 mg/2 mL), (4) homocysteine-MPCs (c = 4.7 mg/2 mL and (5) N-acethyl-L-cysteine-MPCs (c = 5.1 mg/2 mL. Inset: Kinetics traces for: (1) homocysteine-MPCs, (2) homocysteine used as electron donors (concentrations of electron donor molecules identical)

MA-MPCs is more efficient in comparison to co-initiation observed for free mercaptoamino acid acting as a free molecule. This behavior can be attributed firstly to the specific interaction of sulfur electrons with surface plasmon electrons that make an electron transfer from mercaptoamino acid to excited electron acceptor more efficient, or to a high concentration of electron donor in the ligand shell.

ACKNOWLEDGMENTS

This work was supported by the Ministry of Science and Higher Education, grant No N N204 054535.

REFERENCES

1. a) Pączkowski J., Neckers D. C.: "Photoinduced Electron Transfer Initiating Systems for Free Radical Polymerization. In Electron Transfer in Chemistry" (Ed. Gould I. R.), Wiley-VCH, New York 2001, vol 5, pp. 516—585. b) Reiser A.: "In Photoreactive Polymers, the Science and Technology of Resists", Wiley, New York 1989.
2. Gupta S., Gupta N., Neckers D. C.: *J. Polym. Sci. Part A: Polym. Chem.* 1982, **20**, 147.
3. Angiolini L., Caretti D., Carlini C., Lelli N., Rolla P. A.: *J. Appl. Polym. Sci.* 1993, **48**, 1163.
4. Fouassier J. P., Ruhlmann D., Zahouily L., Angiolini L., Carlini C., Lelli N.: *Polymer* 1992, **33**, 3569.
5. Angiolini L., Caretti D., Salatelli E.: *Macromol. Chem. Phys.* 2001, **201**, 2646.
6. Allonas X., Fouassier J. P., Angiolini L., Caretti D.: *Helvetica Chimica Acta* 2001, **84**, 2577.
7. Pączkowska B., Pączkowski J., Neckers D. C.: *Polimery* 1994, **39**, 527.
8. Templeton A. C., Wuelfing W. P., Murray R. W.: *Acc. Chem. Res.* 2000, **33**, 27.
9. Thomas K. G., Kamat P. V.: *Acc. Chem. Res.* 2003, **36**, 888.
10. Goodman C. M., Rotello V. M.: *Mini-Rev. Org. Chem.* 2004, **1**, 103.
11. Novak J. P., Brousseau L. C., Vance F. W., Johnson R. C., Lemon B. I., Hupp J. P., Feldheim D. L.: *J. Am. Chem. Soc.* 2000, **122**, 12 029.
12. MacBeath G., Schreiber S. L.: *Science* 2000, **289**, 1760.
13. Choi I. S., Langer R.: *Macromolecules* 2001, **34**, 5361.
14. Yoon K. R., Lee K.-B., Chi Y. S., Yun W. S., Joo S.-W., Choi L. S.: *Adv. Mater.* 2003, **15**, 2063.
15. Dyer D. J., Feng J., Schmidt R., Wong V. N., Zhao T., Yagci Y.: *Macromolecules* 2004, **37**, 7072.
16. Shan J., Nuopponen M., Jiang H., Vitala T., Kauppinen E., Kontturi K., Tenhu H.: *Macromolecules* 2005, **39**, 2918.
17. Neckers D. C., Hassoon S., Klimtchuk E.: *J. Photochem. Photobiol. A: Chem.* 1996, **95**, 33.
18. Polykarpov A. Y., Hassoon S., Neckers D. C.: *Macromolecules* 1996, **29**, 8274.
19. Tanabe T., Torres-Filho A., Neckers D. C.: *J. Polym. Sci. Part A: Polym. Chem.* 1995, **33**, 1691.
20. Murthy S., Bigioni T. P., Wang Z. L., Khoury J. T., Whetten R. L.: *Mater. Lett.* 1997, **30**, 321.
21. Kang S. Y., Kim K.: *Langmuir* 1998, **14**, 226.
22. Roper T. M., Lee T. Y., Guymon A. C., Hoyle C. E.: *Macromolecules* 2005, **38**, 10 109.

23. Roper T. M., Guyman C. A., Hoyle C. E.: *Rev. Sci. Instrum.* 2005, **76**, 054102.
24. Paczkowski J., Krzekotowski J., Strożecki S.: *Pomiary, Automatyka, Kontrola* 1978, **26**, 8250.
25. Hostetler M. J., Green S. J., Stokes J. J., Murray R. W.: *J. Am. Chem. Soc.* 1996, **118**, 4212.
26. Hostetler M. J., Templeton A. C., Murray R. W.: *Langmuir* 1999, **15**, 3782.
27. Daniel M.-C., Astruc D.: *Chem. Rev.* 2004, **104**, 293.
28. Evanoff D. E., Chumanov G. J.: *J. Phys. Chem. B.* 2004, **108**, 13 957.
29. Jędrzejewska B., Pietrzak M., Ścigalski F., Tomczyk Ż., Pączkowski J.: *Mater. Lett.* 2008, **62**, 4260.
30. Stellacci F., Bauer C. A., Meyer-Friedrichsen T., Wenseleers W., Mardeer S. R., Perry J. W.: *J. Am. Chem. Soc.* 2003, **125**, 328.
31. a) Kucybała Z., Pietrzak M., Pączkowski J.: *Chem. Mater.* 1998, **10**(11), 3555. b) Kabatc J., Pietrzak M., Pączkowski J.: *J. Chem. Soc. Perkin Trans.* 2002, **2**, 287. c) Jędrzejewska B., Marciniak A., Paczkowski J.: *Mater. Chem. Phys.* 2008, **111**, 400. d) Kabatc J., Jędrzejewska B., Pączkowski J.: *J. Polym. Sci. Part A: Polym. Chem.* 2006, **44**, 6345. e) Kabatc J., Kaczorowska M., Jędrzejewska B., Pączkowski J.: *J. Appl. Polym. Sci.* 2008, **108**, 1636.
32. Kabatc J., Jędrzejewska B., Pączkowski J.: *J. Polym. Sci. Part A: Polym. Chem.* 2003, **41**, 3017.
33. Kabatc J., Jędrzejewska B., Pączkowski J.: *J. Appl. Polym. Sci.* 2006, **99**(1), 207.
34. Zhang S., Li B., Tang L., Wang X., Liu D., Zhou Q.: *Polymer* 2001, **42**, 7575.

Received 19 III 2010.